Polymer architecture effects on poly(N,N-Diethyl acrylamide)-b-poly(ethylene glycol)-b-poly(N,N-diethyl acrylamide) thermoreversible gels and their evaluation as a healthcare material

Polymer architecture effects on poly(N,N-diethyl acrylamide)-*b*-poly(ethylene glycol)-*b*-poly(N,N-diethyl acrylamide) thermoreversible gels and their evaluation as a healthcare material

*Peter J. Haddow,[1] Marcelo A. da Silva,[1] Daulet B. Kaldybekov;[2,3] Cecile A. Dreiss,[4] Ewelina Hoffman,[1] Victoria Hutter,[1] Vitaliy V. Khutoryanskiy,[2,3] Stewart B. Kirton,[1] Najet Mahmoudi,[5] William J. McAuley,[1] and Michael T. Cook.[1]**

Dr Peter J. Haddow, Dr Marcelo A. da Silva, Dr Ewelina Hoffman, Dr Victoria Hutter, Dr Stewart B. Kirton, Dr William J. McAuley, Dr Michael T. Cook.

Research Centre in Topical Drug Delivery and Toxicology, School of Life and Medical Sciences, University of Hertfordshire, Hatfield, Hertfordshire, AL10 9AB, U.K.

Dr Daulet B. Kaldybekov, Professor Vitaliy V. Khutoryanskiy

School of Chemistry, Food and Pharmacy, University of Reading, Reading, Berkshire, RG6 6UR, U.K.

Department of Chemistry and Chemical Technology, Al-Farabi Kazakh National University, 050040 Almaty, Kazakhstan

Dr Cecile A. Dreiss

Institute of Pharmaceutical Science, King′s College London, Franklin-Wilkins Building, 150 Stamford Street, London, SE1 9NH, U.K.

Dr Najet Mahmoudi

ISIS Neutron and Muon Source, STFC, Rutherford Appleton Laboratory, Didcot, OX11 0QX, U.K.

Corresponding Author

*m.cook5@herts.ac.uk

ABSTRACT

Thermoreversible gels which transition between liquid-like and solid-like states when warmed have enabled significant novel healthcare technologies. Poly(N,N-diethyl acrylamide) (PDEA) is a thermoresponsive polymer which could be used as a trigger to form thermoreversible gels, however its use in these materials is limited and crucial design principles are unknown. Herein copolymers with the structure PDEA-*b*-poly(ethylene glycol) (PEG)-*b*-PDEA were synthesized to give four block copolymers with varied molecular weight of PDEA and PEG blocks. Rheometry on solutions of the block copolymers revealed that high molecular weight PEG blocks were required to form thermoreversible gels with predominantly solid-like behaviour. Furthermore, small-angle X-ray scattering elucidated clear differences in the nanostructure of the copolymer library which can be linked to distinct rheological behaviours. A thermoreversible gel formulation based on PDEA (20 kDa)-*b*-PEG (10 kDa)-*b*-PDEA (20 kDa) was designed by optimising the polymer concentration and ionic strength. It was found that the gel was mucoadhesive, stable and non-toxic, as well as giving controlled release of a hydrophobic drug. Overall, this study provides insight into the effect of polymer architecture on the nanostructure and rheology of PDEA-*b*-PEG-*b*-PDEA and presents the development of a highly functional thermoreversible gel with high promise for healthcare applications.

KEYWORDS: Hydrogel, stimuli-responsive polymers, mucoadhesion, *in situ* gels, drug delivery

1. Introduction

Thermoreversible gels may switch their state from a low viscosity solution to a gel dependent upon temperature. Engineering these materials so that the sol-gel transition occurs upon warming may be achieved by exploiting polymers with lower critical solution temperatures (LCSTs).[1,2] This phenomenon manifests as a solvophilicity when T<LCST but a relative solvophobicity when T>LCST, which in homopolymers is typically accompanied by a coil-to-globule transition and higher order mesoglobular states.[3,4] Thermoreversible gels may be achieved in these systems when the polymer exhibiting an LCST is covalently bonded to a polymer chain exhibiting solvophilicity over all temperature investigated such that the LCST drives the formation of an amphiphilic state accompanied by self-assembly and/or polymer

entanglements to form a percolating gel phase.[1] The triggering of this gel phase by gentle heating presents opportunity in applications such as drug delivery,[2] bioprinting[5] and tissue engineering,[6] particularly where this transition (T_{gel}) occurs between 25 and ca 37 °C such that *in situ* gel formation is achieved with exposure to the body's heat.

One thermoresponsive polymer is poly(N,N-diethyl acrylamide) (PDEA)[7] which exhibits an LCST of ca. 33 °C,[8] and as such is attractive to design thermoreversible gels with *in situ* gelation potential. However, unlike the structurally-related poly(N-isopropyl acrylamide) (PNIPAM),[9] studies of PDEA are limited.[8] PDEA exhibits relative insensitivity to concentration, with the LCST dropping from 34 to 32 °C when concentration is increased from 0.5 to 4 wt%, which stabilises at 32 °C at concentrations above this.[8] The LCST may be further manipulated by additives, rising by up to ca. 3 °C with the addition of sodium dodecyl sulfate and reducing by up to ca. 20 °C with the addition of sodium chloride due to the electrolyte's "salting-out" effect.[8] PDEA also exhibits a dependency of the LCST with molecular weight, with minor (<2 °C) suppression of cloud points with increasing M_w.[10] This ability to make precision manipulation to the LCST further supports PDEA as a functional material for thermoreversible gel design, however it remains underexploited and unoptimised. To the authors' knowledge, only a single thermoreversible gel using PDEA is reported, a PDEA-poly(acrylic acid)-PDEA copolymer which formed gels at concentrations as low as 3 wt%, far lower than the widely-used Poloxamer 407 gels.[11,12] However, these materials had the disadvantage that T_{gel} occurred at 60 °C and are therefore not of relevance for many biomedical applications. Poly(ethylene glycol) (PEG)-*b*-PDEA materials have been prepared[13] which are capable of self-assembling upon increase in temperature, but no gelation was reported. It was hypothesised that PDEA-*b*-PEG-*b*-PDEA systems would be capable of undergoing thermoreversible gelation due to the ability of triblock copolymers to form flower-like micelles, which may then be bridged by the unimer chain to drive gel phase formation, as observed for PNIPAM-*b*-PEG-*b*-PNIPAM.[14,15]

Within this study, the thermoreversible gelation of aqueous PDEA-*b*-PEG-*b*-PDEA solutions was explored as a function of molecular weight, varying PDEA M_n from ca 10 to 20 kDa and PEG from ca 5 to 10 kDa, using small-angle X-ray scattering (SAXS) to elucidate the morphology of the aggregates present in solution. These thermoreversible gels were then optimised with respect to T_{gel} and gel strength by manipulation of architecture, polymer concentration, and salt concentration to give a highly-functional material with promising

applications in healthcare. This material was then explored for topical drug delivery of both hydrophilic and hydrophobic molecules.

2. Materials and methods

2.1 Materials

N,N-diethyl acrylamide (DEA) (99 %) and progesterone (99 %) were purchased from Sigma-Aldrich (U.K.). Tris[2-(dimethylamino)ethyl]amine (Me_6TREN) (99 %), 2-Bromoisobutyryl bromide (BiBB) (97 %) and copper (I) chloride (CuCl) (99.9 %) were purchased from Alfa Aesar (U.K.). Isopropyl alcohol (iPA) (99 %), HPLC grade acetonitrile, sodium chloride (NaCl) (99.5 %), potassium hydroxide (KOH) (99%) and absolute ethanol (99 %) were purchased from Fisher Scientific (U.K.). Dimethylaminopyridine (DMAP) (97 %), fluorescein sodium salt (NaFl), Poloxamer 407, Poloxamer 188 and polyethylene glycol (PEG) 10 kDa were purchased from Sigma-Aldrich (U.K.). PEG 4 kDa (determined by ^{1}H NMR to have M_n of 5 kDa)[14] was purchased from Fluka (U.K.). Aluminium oxide, neutral, Brockmann I, potassium phosphate monobasic monohydrate (99 %) and tenofovir disoproxil fumarate (98 %) were purchased from Acros Organics (U.K.). Dialysis tubing with a molecular weight cut off (MWCO) of 3500 Da was purchased from Medicell Membrane Ltd (U.K.) and soaked in deionised H_2O for at least 1 h before use. GPC EasiVial poly(methyl methacrylate) (PMMA) mixed standards were purchased from Agilent (U.K.). Dulbecco's Modified Eagle's Medium - high glucose with 4500 mg/L glucose, L-glutamine, sodium pyruvate and sodium bicarbonate (DMEM), Fetal Bovine Serum (FBS), L-Glutamine and Penicillin-Streptomycin (Pen-Strep) were purchased from Sigma-Aldrich (U.K.) and used as purchased. Immortalised human keratinocytes (HaCat) cells were purchased from ThermoFisher Scientific (U.K.). CytoTox-ONE™ Homogeneous Membrane Integrity Assay (LDH) and CellTiter 96® AQueous One Solution Cell Proliferation Assay (MTS) were purchased from Promega (U.K.) and used as per the manufacture's instruction. Deionised H_2O was used in all experiments. All reagents were used as supplied.

2.2 Synthesis and characterisation of PDEA-b-PEG-b-PDEA copolymers

Macroinitiators of 5 and 10 kDa PEG were synthesised and purified as described previously.[14] The reagents and quantities and experimental conditions used for the synthesis of tri-block

copolymers by atom transfer radical polymerisation (ATRP) are shown in SI (table S1). The PEG macro-initiator, ligand (Me_6TREN) and DEA were placed in a round-bottom flask and dissolved in a 1:1 water:MeOH mixture. Copper(I) bromide was added to a separate flask. Both flasks were then sealed and degassed with nitrogen purge for 30 min. After degassing, the solution containing monomer, macroinitiator and ligand was transferred to the copper(I) bromide flask via a degassed syringe. The flask was then stirred at room temperature for 24 h. It has been reported that removal of copper by neutral alumina alone causes copper-related cytotoxicity, which can be eliminated by passage of sample through neutral alumina and dialysis.[16] Therefore, all copolymers were passed through alumina and dialysed for purification. Yields were > 86 % in all cases (SI, Table S1). These polymers are assigned identifiers based on the molecular weight in kDa of the constituent blocks, namely A10-B5-A10, A20-B5-A20, A10-B10-A10, and A20-B10-A20.

^{1}H NMR was performed on an Oxford Instrument ECA600 600 MHz NMR spectrometer with Delta 4.3.6 software. All samples were measured in D_2O. The M_n of triblock copolymers was calculated from ^{1}H NMR. The ratio of the PEG peak integral (3.5 ppm) to that of the DEA proton peaks was used to determine M_n, given that the degree of polymerisation of PEG is known.[14] An Agilent 12600 Infinity II GPC equipped with a refractive index (RI) detector was used to characterise triblock copolymers, determining ~~Đ~~ and confirming monomodality. A Phenomenex Phenogel 10 µm 10E5 Å column was used with DMF with 0.1 % LiBr as an eluent, at a flow rate of 0.4 mL/min with the column and detector held at 30 °C. The GPC was calibrated with Agilent Easivial PMMA standards with M_n ranging from 370 to 364000 Da.

2.3 Rheological evaluation of 20 % (w/v) solutions of PDEA-b-PEG-b-PDEA

All rheology experiments were performed on a TA AR 1500 ex shear rheometer with a Peltier temperature control unit (±0.1 °C) using rheology advantage software and a 40 mm parallel plate. The gap was 650 µm. A solvent trap was used to prevent evaporation. All samples were prepared at the stated composition in aqueous solution and left overnight in the fridge before performing rheometry. All experiments were repeated 3 times.

Oscillatory shear stress sweep (OSS) experiments were performed at 20 °C between 1 to 100 Pa. The linear viscoelastic region (LVR) was identified as the region before the increase in oscillatory stress caused both storage (G′) and loss (G″) moduli to decrease, which was

determined to be the yield stress. Frequency sweeps were conducted between 0.1 and 10 Hz at a stress of 1 Pa.

Temperature ramps were performed at 1 Pa of oscillatory stress and a frequency of 1 Hz, with an increase in temperature from 20 to 70 °C at a rate of 2 °C per minute. The T_{gel} was determined at the cross-over point between G′ and G″, a criterion widely used in the literature [17] and the gel "strength" was taken as the maximum value of G′ reached across the temperature range. Reversibility of this transition was explored by cycling the sample between 20 at 37 °C, holding for 60 s at each temperature with a pre-measurement equilibration time of 120 s whenever the temperature was altered. Time-dependency of gelation was determined by holding the sample at 20 °C for 60 s, then transitioning to 37 °C and keeping the temperature fixed for 240 s. A stress of 1 Pa and frequency of 1 Hz was used in these experiments.

2.4 Small-Angle X-Ray Scattering (SAXS) measurements of copolymer solutions

Samples of each copolymer were prepared at 5 wt% in deionised water. SAXS measurements were performed on a Nano-inXider SAXS/WAXS instrument (Xenocs, Sassenage, France) at the Materials Characterization Laboratory of the ISIS Neutron and Muon source (STFC, Rutherford Appleton Laboratory, Didcot, UK). The setup is equipped with a micro-focus sealed-tube Cu 30W/30 µm X-ray source (Cu K-α, λ = 1.54 Å) and two Dectris Pilatus 3 hybrid pixel detectors, covering scattering vector q-ranges ($q = 4\pi\lambda\sin(\theta/2)$, where λ is the wavelength of the incident beam and θ is the scattering angle) of 0.0045 $Å^{-1}$ to 0.37 $Å^{-1}$ and 0.3 $Å^{-1}$ to 4.1 $Å^{-1}$ for SAXS and WAXS, respectively. Scattering from the samples and water was collected in 1 mm glass thermalized capillaries at temperatures between 30 and 60 °C. Data reduction (azimuthal averaging, buffer subtraction, absolute scaling) was carried out using the Foxtrot software. SAXS data was fitted using Sasview 4.2.2 software.

The scattering intensity $I(q)$ can be written as follow:

$$I(q) = A(P(q)_A S(q)_A) + BKG$$

where, A is a scale factor, $P(q)$ is the form factor of the scattering object, $S(q)_A$ is the corresponding structure factor and BKG is the background.

If more than one scattering object is present or the object studied has a hierarchical structure that generates scattering at distinct length scales, the expression can be extended to include further terms.

For this work, the polymer constructs, in general, give rise to two scattering components, one derived from their supramolecular structure and another from the polymeric chains. Therefore, the $I(q)$ expression used was extended to:

$$I(q) = Scale(A(P(q)_A S(q)_A)) + B(P(q)_{PGC}) + BKG$$

where, *Scale*, *A* and *B* are scale factors, , $P(q)_A$ is the form factor for the model *A*, $S(q)_A$ is the corresponding structure factor, $P(q)_{PGC}$ is the form factor model of polydisperse polymer coils, and *BKG* is the background. [18]

The SAXS data were fitted as follow: A10-B5-A10, either as polymeric Gaussian coils[18] or with a cylinder model.[19,20] A10-B10-A10, either polymeric Gaussian coils,[18] ellipsoids[21,22] plus polymeric Gaussian coils[18] or sphere[23] model for form factor and hard spheres[24,25] for the structure factor as needed. A20-B5-A20, either polymeric Gaussian coils[18] or spheres[23] models. A20-B10-A20, either polymeric Gaussian coils,[18] ellipsoids[21,22] plus polymeric Gaussian[18] coils or sphere[23] models for form factors and hard spheres structure factor as needed.[25,26]

2.5 Dynamic light scattering

All dynamic light scattering (DLS) experiments were performed on a Malvern Zetasizer Nano ZS with a scattering angle of 173 °. 1 mg/mL polymer solutions were prepared in deionised water and stored in the fridge overnight before use. Samples were then filtered through a 1 µm syringe filter and size measurements were taken at 50 °C as a comparator measurement above the thermal transition in all systems. A 5-minute equilibration period was used before each measurement, which was conducted in triplicate.

2.6 Investigating the saturation solubility of progesterone and tenofovir disoproxil fumarate in A20-B10-A20 solution

30 % A20-B10-A20 in 0.3 M NaCl was prepared and stored in the fridge overnight. Following this, 1 mL of the polymer solution or water was transferred to a vial and progesterone or

tenofovir disoproxil fumarate (ca 5 mg) was added. The solutions were then placed in a water bath at 25 or 37 °C and allowed to stir for 24 h. If the resultant solution was clear, drug was again added and the sample left for 24 h in the water bath with constant stirring. This process was repeated until the solution remained turbid for 24 h. Excess drug was then removed by centrifugation (10 min at 14500 rpm) ("high speed microcentrifuge", Four E's) and the clear supernatant was analysed by HPLC using validated protocols described elsewhere.[14] Each experiment was performed in triplicate.

2.7 Investigating the release of progesterone and tenofovir disoproxil fumarate in A20-B10-A20 solution

The release of progesterone and tenofovir disoproxil fumarate from the 30 % A20-B10-A20 solution in 0.3 M NaCl was investigated using Franz diffusion cells (Soham Scientific, average bore size 174 mm^2) equipped with a cellulose membrane (Medicell, MWCO 3.5 kDa) at both 25 and 37 °C. The receiver fluid was 10 mL phosphate buffer saline (PBS). The release of 50 µg/mL progesterone or tenofovir disoproxil fumarate in the polymer solution was investigated under sink conditions, by ensuring that drug in the receiver fluid could not exceed 10 % of the drugs' saturation solubilities. The cells were placed into a water bath for 30 min prior to the experiment to reach the required temperature (25 or 37 °C). Cells were dosed with 200 µL of sample and the release of drug measured at regular intervals by sampling receiver fluid (1000 or 200 µL for the progesterone and tenofovir disoproxil fumarate respectively). The receiver fluid was replaced with an equal volume of pre-warmed PBS. The samples were analysed by HPLC using established protocols.[14] The experiment was repeated 4 times.

2.8 Culture of HaCaT cells

The human keratinocyte (HaCaT) cell line was used between passage numbers 2 and 20 from purchase. Cells were maintained in T75cm^2 cell culture flasks containing 15 mL Dulbecco's Modified Eagle's Medium (DMEM) with 10% v/v heat-inactivated foetal bovine serum (FBS) and supplemented with 100 IU/mL pencillin, 100 µg/mL streptomycin solution and 2 mM L-glutamine. Cells were cultured in a humidified atmosphere at 37 °C with 5% v/v CO_2. Cells were passaged using 5 mL 0.25% w/v trypsin-EDTA solution once weekly when 90% confluent and subcultured at a ratio of 1:10. For experiments, cells were seeded at a density of

1 x 10^5 cells/well on 96 well tissue culture plates in 100 µL of complete cell culture medium and were cultured for 4 days prior to experimentation.

2.9 Cytotoxicity testing of triblock copolymers on HaCat cells

On the day of cytotoxicity assessment, cell culture medium was removed and replaced with 100 µL cell culture medium containing 10 mg/mL copolymer. Controls of untreated cells and cells treated with 0.1 % v/v Triton-X 100 were included in each experiment. Cells were incubated at 37 °C in 5 % v/v CO_2 for 2 h and assessed for viability. Four replicates of the condition were used for each sample.

The CytoTox-ONE™ Homogenenous Membrane Integrity assay kit was used to quantify the extracellular concentration of lactate dehydrogenase (LDH) which arises due to the presence of pores in the cell membrane, one indicator of cytotoxicity. After 2 h of polymer exposure, 50 µL of cell supernatant was removed from each well and transferred to a black 96 well plate. To this, 50 uL of CytoTox-ONE™ Reagent (1:1 ratio) was added and cells were incubated in the dark for 10 minutes at room temperature (~19 °C) before the addition of 25 µL of stop solution. Fluorescence was measured immediately using a Promega Glomax Multi Detection System fluorescence plate reader with excitation wavelength of 560 nm and an emission wavelength of 590 nm. The data was then expressed as a percent cytotoxicity compared to positive control cells dosed with 0.1 % v/v Triton-X 100 (Equation 1).

$$\text{Membrane Leakage (\%)} = \frac{(\text{Dosed Cells} - \text{Background})}{(\text{Positive Control} - \text{Background})} \text{ X } 100 \qquad \text{(Equation 1)}$$

The CellTiter96 Aqueous One Solution Cell Proliferation assay kit was used according to manufacturer's instruction to assess mitochondrial activity of the cells. This is used in combination with LDH assay as an additional supporting measure of cell viability where pores may be present in the membrane, detectable by LDH assay, but of insufficient size to cause the membrane to be destroyed. After a 2 h exposure to polymers, 50 µL of supernatant was removed and 10 µL of CellTitre ONE Reagent was added to the remaining 50 µL cell sample (1:5 dilution). Samples were incubated for 2 h in a humidified incubator at 37 °C, 5% v/v CO_2. Samples were analysed for absorbance at 492 nm using the CARIOstar microplate reader

(BMG Labtech). The data was expressed as percent metabolic activity compared to untreated cells in culture medium as a negative control (Equation 2).

$$\text{Metabolic Activity (\%)} = \frac{(\text{Dosed Cells} - \text{Background})}{(\text{Untreated Cells} - \text{Background})} \text{ X } 100 \qquad \text{(Equation 2)}$$

2.10 Ex vivo retention studies on porcine vaginal tissues

Porcine vaginal tissues were received from P.C. Turner Abattoirs (Farnborough, UK) immediately after slaughter of the animals and were used for evaluating the mucoadhesive properties of the formulations using a previously described method.[27,28] The tissues were carefully excised to yield approximately 2×2 cm pieces, avoiding contact with the internal mucosa, which were then used in the experiments. The dissected vaginal tissue was mounted on a glass slide with mucosal side facing upward and pre-rinsed with 1 mL of vaginal fluid simulant (VFS; pH 4, preparation described in SI). Experiments were performed with the vaginal tissues maintained at 37 °C and 100 % relative humidity in an incubator. Aliquots (200 µL) from 30 wt % PDEA-PEG-PDEA prepared in 0.3 M NaCl solution; 20 wt % Poloxamer 407 and 20 wt% Poloxamer 188 solutions prepared in deionised water containing 0.2 mg/mL fluorescein sodium salt (NaFl) and a control of NaFl (0.2 mg/mL) solution were deposited onto a mucosal surface and rinsed with VFS at a constant flow rate of 0.3 mL/min using a syringe pump. Fluorescence images of a vaginal tissue were taken using Leica MZ10F stereo-microscope (Leica Microsystems, UK) with Leica DFC3000G digital camera at 1.6× magnification with 10 ms exposure time (gain 1.0×), fitted with a GFP filter. The microscopy images were then analysed with ImageJ software by measuring the pixel intensity after each irrigation with VFS. The pixel intensity of the blank samples (vaginal mucosa without test material) was subtracted from each measurement and data were converted into values of intensity. All measurements were performed in triplicate.

2.11 Investigating the stability of A20-B10-A20 under ambient, refrigerated and accelerated storage conditions.

The stability of A20-B10-A20 copolymer was assessed over 12 weeks. Polymer solutions at 30 % w/v in 0.3 M NaCl were prepared in HPLC vials sealed with parafilm and stored in the refrigerator (4 °C) or at ovens set at 25 and 40 °C representing ambient temperature and

accelerated storage conditions, respectively. Each week three vials under each storage condition were lyophilised and the molecular weight determined by GPC.

2.12 Statistical analysis

Statistical analysis of data from mucoadhesion studies, i.e. mean values ± standard deviations, were calculated and assessed for significance using two-tailed Student's *t*-test and a one-way analysis of variance (ANOVA) followed by Bonferroni post hoc test using GraphPad Prism software (version 7.0), where $p < 0.05$ was considered as statistically significant.

3. Results and discussion

PDEA-*b*-PEG-*b*-PDEA copolymers were synthesised by ATRP to give a series of samples with molecular weight (in kDa) of each block controlled at two values, namely: A10-B5-A10, A20-B5-A20, A10-B10-A10, and A20-B10-A20. Polymer structure was confirmed by ^{1}H NMR (Figure 1a), which was also used to determine the number average molecular weight of the blocks (Table S2, SI). GPC was used to determine the Đ, which was < 1.4 in all cases, and confirm the absence of residual PEG macroinitiator (Figure 1b,c). GPC also confirms the that PEG macroinitiator was not detectable in the product, with a shift of peak to lower elution times (and thus assumed greater molecular weight). Whilst PEG-*b*-PDEA copolymers have recently been reported in the literature,[13] to our knowledge this is the first reported synthesis of PDEA-*b*-PEG-*b*-PDEA. This is particularly significant where the ABA triblock copolymer architecture gives access to nanostructures unavailable to diblock geometries and is associated with an enhanced ability to form gel phases.[1] It was hypothesised that ABA triblock copolymers of this type should have the ability to act as "loops", "bridges", or "dangling chains" in micellar structures and form percolating gel phases in an analogous manner to telechelic polymers exhibiting solvophilicity in their centre and solvophobicity at their termini.[29]

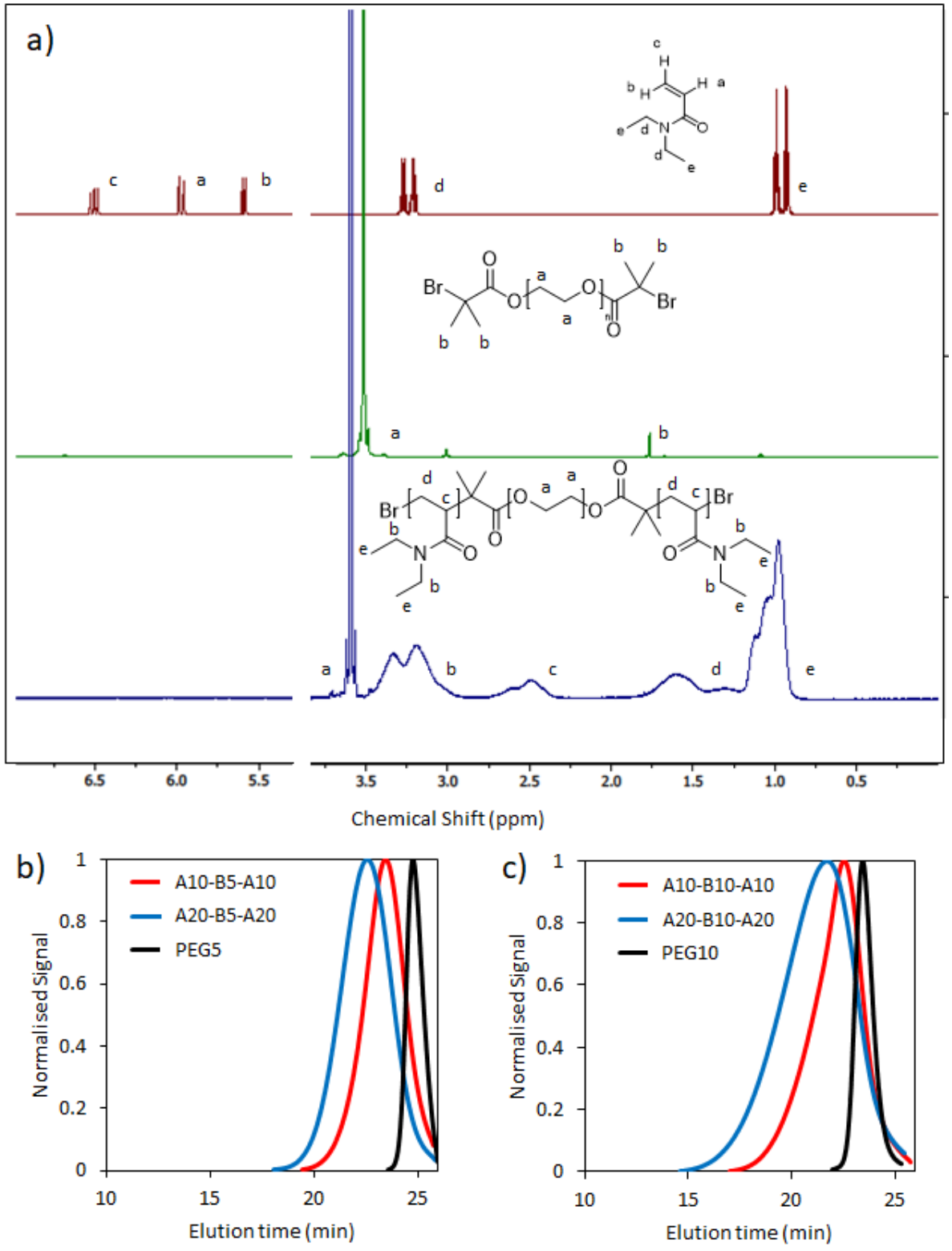

Figure 1. a) ^{1}H NMR spectra of DEA, PEG and an exemplar PDEA-b-PEG-b-PDEA copolymer. GPC traces of copolymers with (b) 5 kDa and (c) 10 kDa PEG "B" blocks.

The potential of the PDEA-b-PEG-b-PDEA copolymers to form thermoreversible gels in aqueous solution was then evaluated by small-amplitude oscillatory shear rheology as a function of temperature at a fixed concentration of 20 % (w/v). In these experiments G′ and G″ are measured as temperature changes at a fixed stress, within the linear viscoelastic region, and a fixed frequency. This ensures that any structures formed within the sample are not altered by high shear. All polymer architectures showed thermothickening from ca. 35-40 °C, increasing in viscosity with temperature above this point (Figure 2). The composition of the polymer induced notably different rheological behaviours in the systems. Samples with 5 kDa central PEG blocks increased in viscosity but exhibited predominantly liquid-like behaviour above the thermal transition, with G″ never exceeding G′. However, when 10 kDa PEG constitutes the "B" block of the ABA copolymer the materials exhibit a thermoresponsive gelation, with G′ exceeding G″, indicating a dominance of solid-like behaviour in the system when heated. The gelation of A10-B10-A10 and A20-B10-A20 occurred at 51.2 ± 1.8 and 45.9 ± 0.5 °C, respectively, indicating that the gelation process occurs at temperatures above the reported LCST of DEA homopolymer, ca 33 °C.[8] This deviation may be the result of several factors. Conjugation to hydrophilic species has been shown to elevate LCST,[1] and it is known that macromolecular transitions continue to evolve above the LCST.[30,31] For example, the degree of phase separation of PNIPAM chains occurs over a broad transition in PNIPAM-*b*-PEG-*b*-PNIPAM copolymers.[30] Thus, nanostructures continue to evolve as heating continues above the LCST, rather than exhibiting a stepwise transition at this temperature. From the materials studied by rheology, A20-B10-A20 was identified as the most promising thermoreversible gel in the library due to its relatively high gel strength of up to 1.5 kPa.

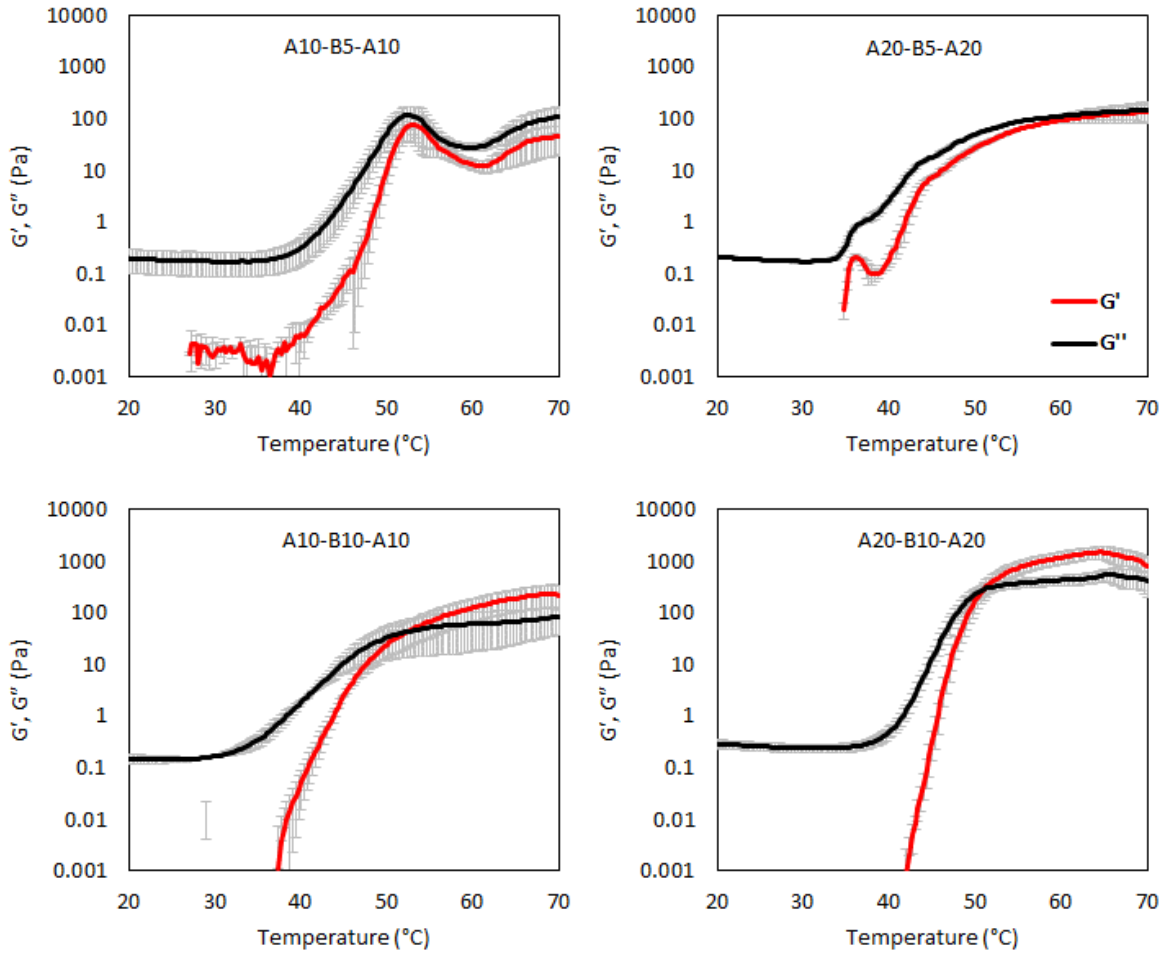

Figure 2. PDEA-b-PEG-b-PDEA copolymer solutions (20 % (w/v) studied by small-amplitude oscillatory shear rheology as a function of temperature, measured at a shear stress of 1 Pa and a frequency of 1 Hz.

The size of assembled structures of PDEA-b-PEG-b-PDEA copolymers in dilute aqueous solutions (1 mg/mL) was probed by dynamic light scattering above the transition temperature (Figure 3) in order to extract differences between the constructs, which could give clues into the mechanisms of gelation in more concentrated systems. The constructs with the larger PEG block, A10-B10-A10 and A20-B10-A20, formed well-defined nanoparticles with 68 nm median hydrodynamic diameter and polydispersity indices of 0.22 and 0.08, respectively. The lower molecular weight 5 kDa PEG copolymers assembled into much larger structures than the 10 kDa PEG constructs, with hydrodynamic diameters of 396 and 531 nm for A10-B5-A10 and A20-B5-A20, respectively.

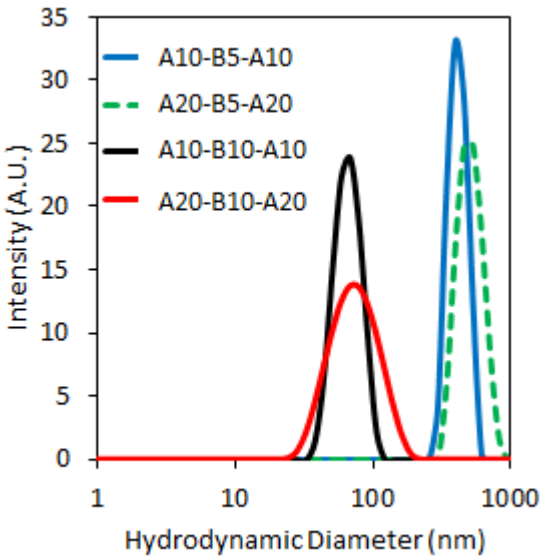

Figure 3. Block copolymer aggregate size distributions in dilute aqueous solutions (1 mg/mL) at 50 °C as determined by dynamic light scattering.

SAXS was employed to further probe the nanostructure of PDEA-*b*-PEG-*b*-PDEA copolymers as a function of temperature. Measurements were taken from 5 wt% solutions in H_2O at 30, 37, 40, 50, and 60 °C to span the range of temperatures covered by rheology and elucidate morphology above and below the transition temperature. All copolymers were investigated, however A20-B5-A20 visually showed evidence of phase separation at elevated temperatures – probably due to the large LCST blocks combined with the short hydrophilic PEG block – hence the data were not analysed. The scattering profiles of all copolymers showed clear structural transitions when warmed above 40 °C (Figure 4), in agreement with the rheology presented in Figure 2. The scattering from A10-B5-A10 system (figure 4a) was fitted with a polydisperse Gaussian coil (PGC) form factor at 30 and 37 °C, indicative of the system behaving as a disperse mixture of polymer chains in a theta solvent.[18] At 40 °C the system was fitted with a cylinder form factor (radius of 6.2 nm), the length of which was outside the length scale resolved by SAXS and is expected to be greater than ca. 80 nm based on the *q* range available. At this temperature a power law form factor (exponent 1.61) was added to the model to fit the high *q* region, which may be a contribution from polymer chains in a good solvent (exponent 1.66), possibly arising from PEG chains in the micellar corona.[32]. At 50 and 60 °C, the data could be described by a cylinder form factor of radii 9.1 and 8.7 nm, respectively. These elongated structures are in agreement with the DLS data that detected very large aggregates. The construct with a larger PEG central block, A10-B10-A10 (Figure 4b) also revealed the presence of Gaussian coils at 30 and 37 °C. At 40 °C, a transition requiring

two form factors was again observed accounting for the presence of PGCs in addition to ellipsoidal objects with polar and equatorial radii of 20.5 and 10.2 nm, respectively. At 50 and 60 °C, A10-B10-A10 data were best described by a spherical form factor with radii of 12.9 and 13.7 nm, respectively, which also required a contribution from a hard sphere structure factor, accounting for inter-particle repulsions.[25,26] A20-B10-A20 copolymers, which bear larger side chains and the same size of PEG central block, followed a similar trend. At 30 °C the scattering data were fitted to a PGC form factor. At 37 °C, assembled structures with an elliptical shape, with polar and equatorial radii of 26.2 and 11.3 nm, respectively, were detected, in addition to polymer coils. The same combination of form factors was used at 40 °C, with the ellipsoids having polar and equatorial radii of 27.5 and 15.7 nm, respectively. At 50 and 60 °C, only the ellipsoid form factor was required to fit the data, giving polar and equatorial radii of 28.5 and 19.1 nm, respectively, at 50 °C and of 27.8 and 19.3 nm at 60 °C, in broad agreement with the hydrodynamic diameter obtained from DLS. The ellipsoidal objects A20-B10-A20 also required the addition of a hard sphere structure factor to fit the data, which is a reasonable approximation for particle shapes that deviate from spheres.[25] Further detail about the models used and parameters obtained from the SAXS analysis can be found in the SI (Tables S3-S5).

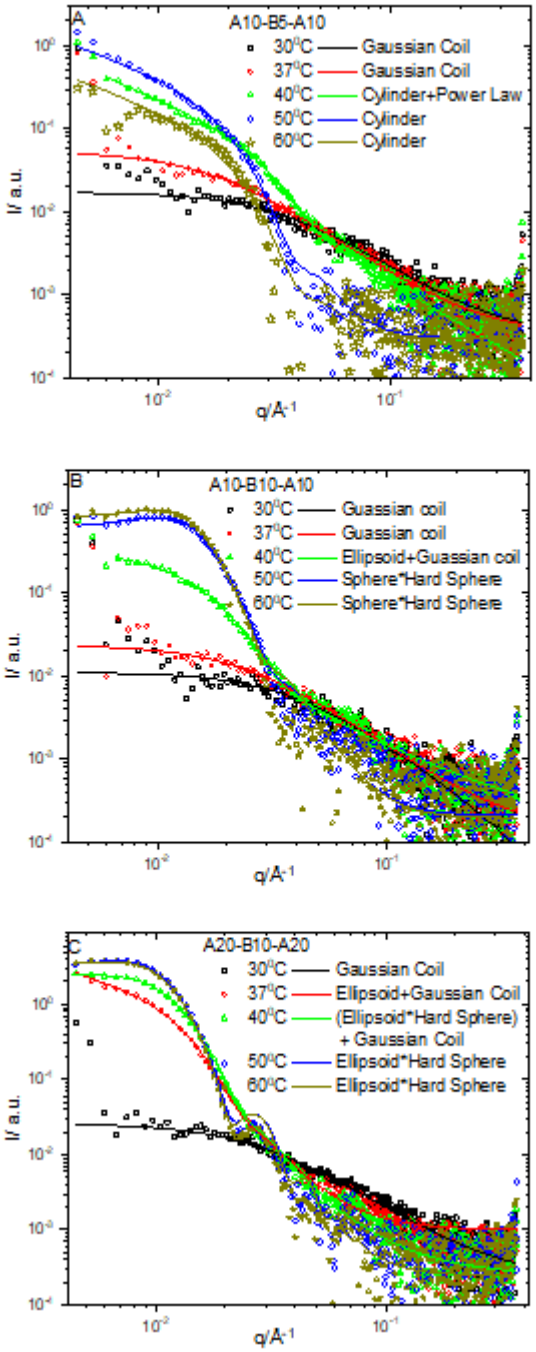

Figure 4. Small-Angle X-Ray Scattering profiles of (a) A10-B5-A10 (b) A10-B10-A10 and (c) A20-B10-A20 PDEA-*b*-PEG-*b*-PDEA copolymers at 5 wt % over the temperature range 30 to 60°C.

In summary, SAXS measurements indicate that the A10-B5-A10, A10-B10-A10 and A20-B10-A20 constructs are present as polymer chains in solution at lower temperatures, which is associated with a low viscosity (Figure 2). When heated, the systems self-assemble into larger

structures, driven by the LCST transition and the association of the relatively hydrophobic PDEA chains, leading to an increase in visco-elasticity (Figure 2). Cylindrical structures are present in the A10-B5-A10 systems (Figure 5) above the transition temperature, which may be rationalised by the classical "molecular packing parameter" theory of surfactants that has been widely applied to self-assembled polymer structures.[33] In brief, the curvature of a micellar aggregate formed by polymeric amphiphiles is greatly dependent upon the area of the headgroup (in this case PEG) relative to the hydrophobic tail groups (PDEA above the LCST). When the relative area occupied by the headgroup is sufficiently small, the curvature necessary to form a sphere that minimises the interface cannot be achieved and cylindrical structures are formed, as seen in constructs with a low M_n PEG, such as A10-B5-A10, which are expected to be quite long as inferred from the DLS. Instead, the A10-B10-A10 constructs assembled into spheres above the LCST. In this case, the headgroup has a larger size and the packing parameter would allow sufficient curvature to thermodynamically favour a spherical shape. Above the LCST, the A20-B10-A20 copolymers assembled into ellipsoids with an aspect ratio of approximately 2:3. In this case, the relative size of the head-to-tail group is lower and again non-spherical structures are formed. Linking these findings to the rheology elucidates an important contribution of particle shape to viscoelasticity. The cylindrical A10-B5-A10 nanostructures form viscous liquids dominated by the dissipative loss modulus ($G''>G'$). However, where spherical and ellipsoidal nanostructures are present, the systems form predominantly elastic gels ($G'>G''$) at higher concentrations. This may be rationalised by longer PEG chains in these systems the aggregates to be bridged by elastically active unimer chains. Whilst an attractive interaction associated with unimer bridges was not detected via SAXS in these dilute solutions, previous SANS studies at high concentrations support their presence.[34] Alternatively, the short chain length of PEG in the A10-B5-A10 and A20-B5-A20 systems may not allow bridge formation between aggregates. In this case, the increased viscosity in the A10-B5-A10 and A20-B5-A20 constructs may be attributed to entanglements of elongated cylinders in a manner akin to the behaviour of wormlike micelles.[35] Interestingly, whilst PEG length is crucial to gelation, no upper limit to this has been identified in the literature, to our knowledge.[14,36–38] Future studies should expand this library to confirm optimal PEG block length at greater degrees of polymerisation. The A20-B5-A20 systems additionally showed evidence of phase separation so their rheology is treated with caution.

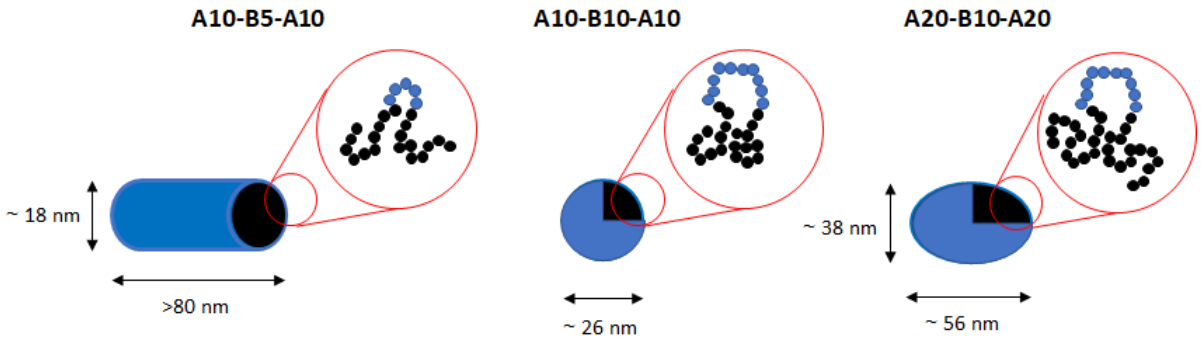

Figure 5. Schematic representation of the self-assembled structures of PDEA-*b*-PEG-*b*-PDEA that form above the LCST.

Cytotoxicity measurements were conducted on human keratinocyte (HaCaT) cells to guide the selection of candidate materials for healthcare applications (Figure 6). There was no evidence of cytotoxicity in either MTS assay, a measurement of mitochondrial activity, or LDH assay, which determines the porosity of the cell membrane when exposed to the A10-B5-A10, A10-B10-A10, or A20-B10-A20 samples. Whilst the dosing interval for these materials was short (2 h), the measurements provide preliminary mitigation of safety risks until optimal materials can be tested under toxicological regimes recognised by regulatory bodies. This testing also provides reassurance that the materials can be used in cell-based applications such as 3D culture or bioprinting.

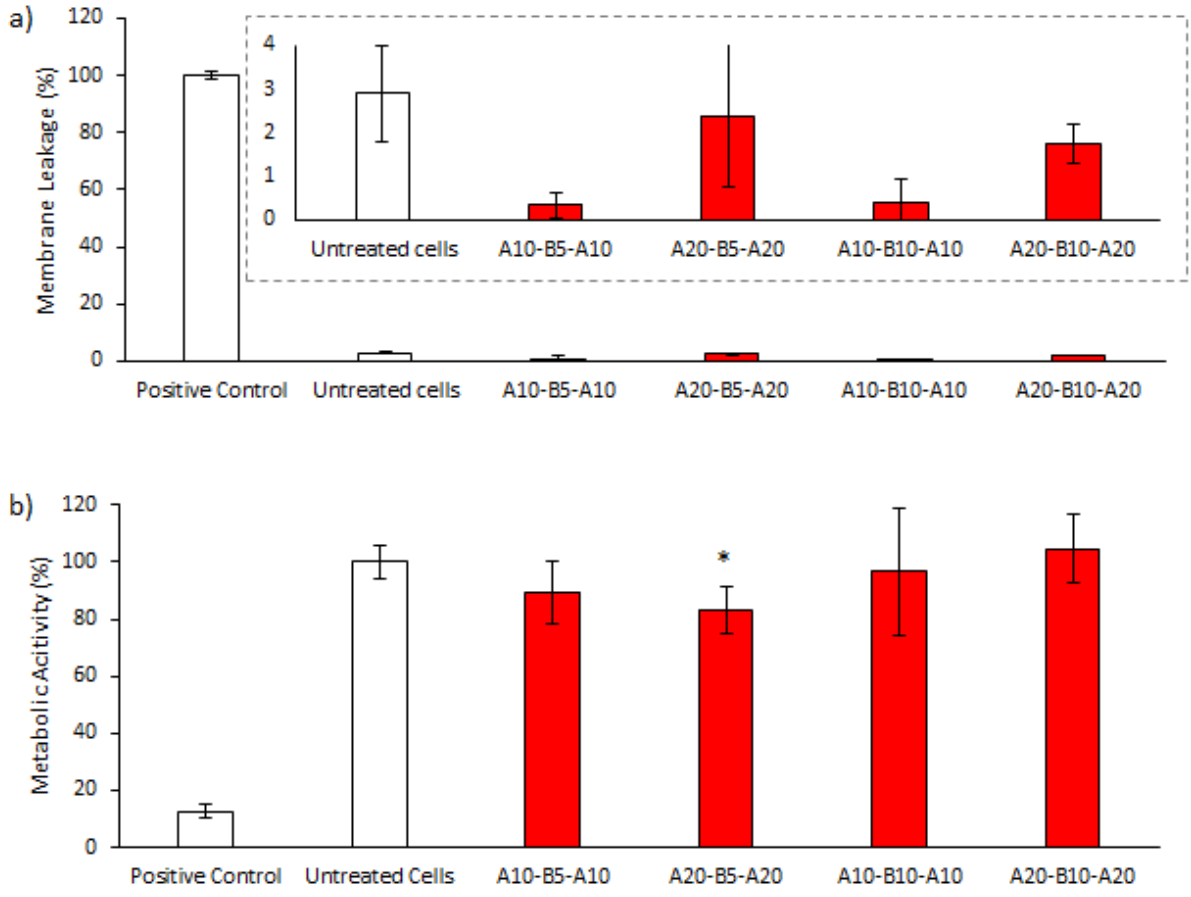

Figure 6. Evaluation of cytotoxicity by LDH (a) and MTS (b) assay showing membrane leakage of LDH and mitochondrial activity, respectively. Cells dosed with 10 mg/mL polymer solution for 2 h prior to evaluation. Positive controls were treated with 0.1 % v/v Triton-X 100. Insert on (a) is expanded to show near-zero values. * designates statistical significance from untreated cells ($p < 0.05$) by one-way ANOVA with Tukey post-hoc (GraphPad Prism, USA). Data is presented as mean ± standard deviation (n = 4).

A20-B10-A20 was selected as the lead thermoreversible gelator for further optimisation due to its high gel strength and apparent cytocompatibility. The drawback of this material thus far is the transition temperature, with gelation not observed until 46 °C. Initially the lowering of this temperature (T_{gel}) was attempted by simply increasing the concentration of the material, where competition for solvent is believed to drive the LCST to lower temperatures in similar systems.[14,39,40] Aqueous solutions of A20-B10-A20 were prepared between 20 and 50 % w/v and evaluated by rheology (Figure S1), as previously described, and the thickening temperature (Tthick), T_{gel} and the maximum value of G′ (G'_{max}) extracted (Figure 7a). It was observed that

T_{gel} decreased from ca 45 to 41 °C when the concentration was increased from 20 to 30 % (w/v), but plateaued above that concentration. Concurrently, G'_{max} increased up to ca 5.8 kPa at 30 % (w/v), plateauing thereafter. The effect of sodium chloride on thermoreversible gel formation was then investigated to attempt to further reduce the LCST below physiological temperature (37 °C) (Figure 7b). A near-linear decrease in T_{gel} with sodium chloride concentration was observed. It is known that sodium chloride can alter the LCST of PNIPAM through the interaction of sodium cations with the oxygen atom in the amide group, which in turn reduces hydration.[41] It is reasonable to assume that this effect is also present in PDEA which is also a poly(N-alkyl acrylamide). The addition of 0.3 M sodium chloride to 30 % w/v A20-B10-A20 solutions gave a thermoreversible gel with T_{gel} occurring at 36 °C, therefore making it an attractive candidate for the design of *in situ* gelators intended to transition between room (ca 25 °C) and body (37 °C internally) temperature (Figure 6c). Hereon, this material is referred to as A20-B10-A20 thermoreversible gel.

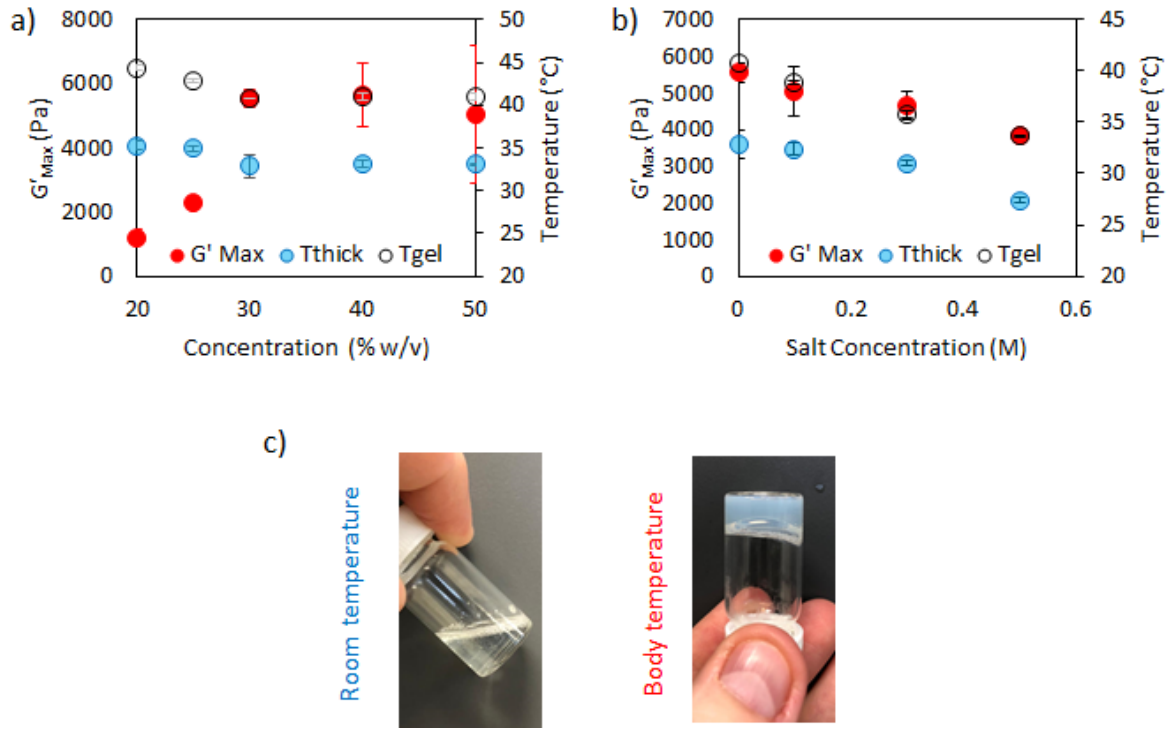

Figure 7. a) Effect of concentration on the transition temperature and maximum gel strength in aqueous solutions of A20-B10-A20. b) Effect of NaCl on these parameters at a set concentration of A20-B10-A20 (30 % (w/v)). c) Image of 30 % (w/v) A20-B10-A20 in 0.3 M NaCl at room (ca 20 °C) and body temperature (after 5 min in a water bath at 37 °C).

A20-B10-A20 thermoreversible gel was subjected to rigorous rheological evaluation to probe its potential as a healthcare material. Oscillatory frequency sweeps (Figure 8a) revealed a low dependence of G′ and G″ on frequency, indicative of a rigid structure which did not undergo structural rearrangements over the test. Amplitude sweeps (Figure 8b) determined a linear viscoelastic region with a reduction in G′ indicative of the onset of yield occurring at 862 Pa, over three-fold higher than the "gold standard" thermoreversible gel of 20% (w/v) Poloxamer 407 which was determined as 256 Pa.[14] This greater yield stress is valuable in applications where the materials are required to retain their shape under shear, such as in topical drug delivery and in maintaining form after bioprinting. The reversibility of the thermal gelation was confirmed by small amplitude oscillatory rheology switching between 25 and 37 °C (Figure 7c), confirming that the rheological behaviour was preserved after a heating-cooling cycle. Finally, the time required for gel formation was investigated by holding the sample at 25 °C then ramping to 37 °C and maintaining the sample at that temperature under a small amplitude. The sample took 67 s to form a gel under these conditions which must be considered in its future applications, however thickening occurred immediately.

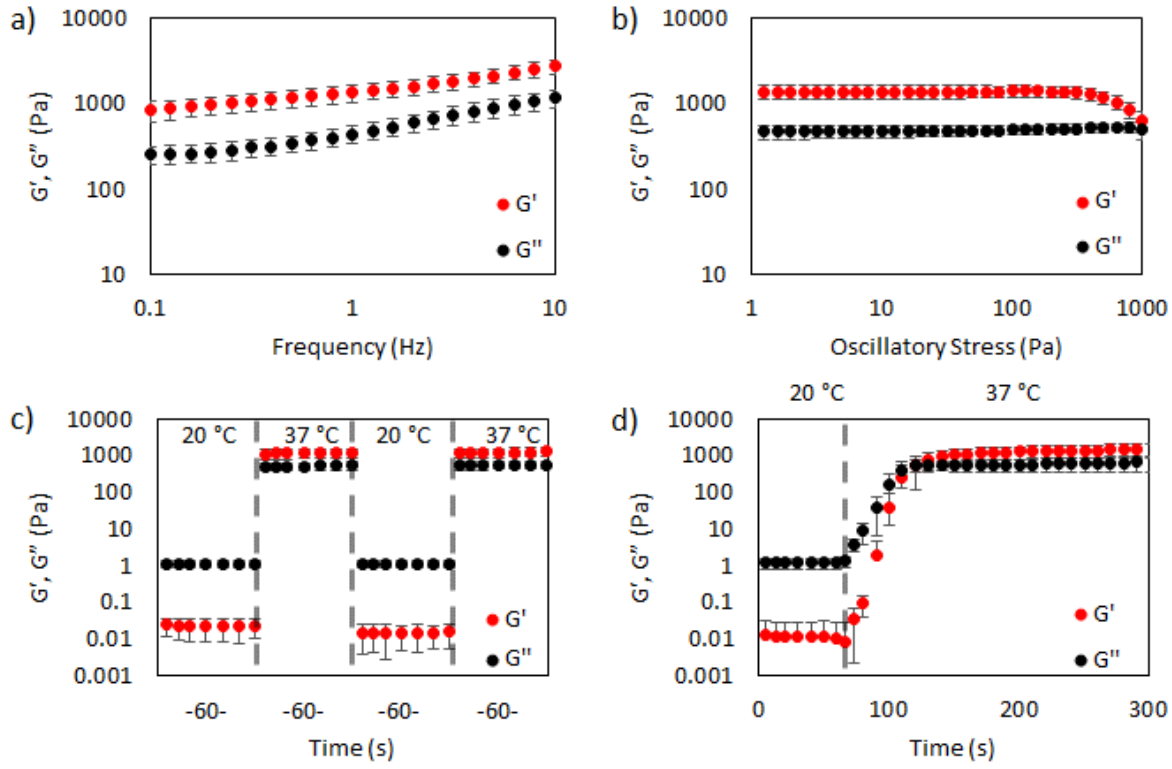

Figure 8. Rheological evaluation of the optimised A20-B10-A20 PDEA-b-PEG-b-PDEA copolymer as a 30 % (w/v) solution in 0.3 M NaCl. (a) Frequency and (b) amplitude sweeps at 37 °C. (c) Reversibility of gelation determined by small-amplitude oscillatory rheology with switching between sol (20 °C) and gel (37 °C) states (please note there was a 120 s equilibration time at each temperature change during which data was not collected). (d) Time taken for gelation to occur determined by holding at 20 °C for 60 s, then switching to 37 °C.

The stability of A20-B10-A20 was assessed in aqueous solution at 4, 25, or 40 °C, reflecting refrigerated storage, storage at room temperature, and an accelerated storage condition, respectively (Figure 9). Accelerated storage at 40 °C aimed to predict longer-term storage at room temperature. GPC analysis demonstrated that at 4 and 25 °C the reduction in number-average molecular weight of A20-B10-A20 was not statistically significant, while at 40 °C there was a significant decrease only by week 12 ($p < 0.05$ by one-way ANOVA with Tukey post-hoc analysis (GraphPad Prism, USA)). GPC traces of A20-B10-A20 remained monomodal with no shoulder (Figure S2), suggesting a reduced likelihood that hydrolysis of the ester moieties between the A and B blocks is a major route of degradation under these conditions. Overall, the A20-B10-A20 copolymer appears stable at and below room temperature in solution for the 12-week study period, supporting its stability during use in pharmaceuticals or cell culture.

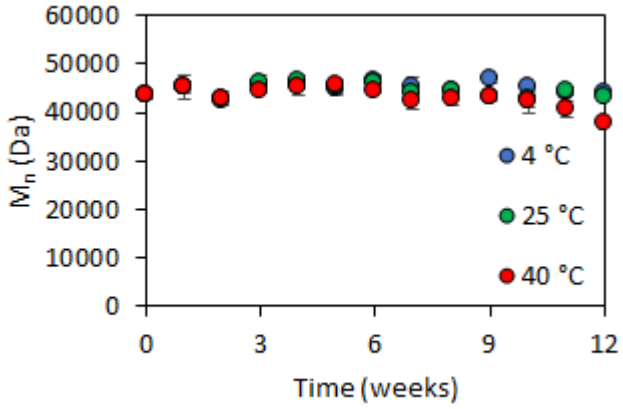

Figure 9. Number-average molecular weight (M_n) of A20-B10-A20 during storage at 4, 25 and 40 °C. Data presented as mean ± standard deviation, n = 3.

The high-performance of the A20-B10-A20 thermoreversible gel makes it an attractive candidate for topical drug delivery to the vagina, where poor retention at this site due to shear forces reduces the efficacy of many semi-solids.[42] Thus, drugs applicable to vaginal drug delivery were incorporated into the thermoreversible gels to evaluate performance in topical drug delivery. Two drugs were investigated for inclusion into the thermoreversible gel, namely progesterone and tenofovir disoproxil fumarate, which have been applied intravaginally for indications including luteal phase support and HIV pre-exposure prophylaxis, respectively.[43,44] Progesterone (clogP = 3.87) is considered to be hydrophobic while tenofovir disoproxil fumarate (clogP = 1.25) is more hydrophilic with saturation solubilities in PBS at 25 °C of 9 ± 1 and 7065 ± 412 µg/mL, respectively, and in PBS at 37 °C of 11 ± 1 and 12269 ± 393 µg/mL, respectively. It was found that the solubility of progesterone was greatly enhanced by inclusion in the A20-B10-A20 thermoreversible gel, particularly above T_{gel}, with progesterone saturation solubilities at 25 and 37 °C of 156 ± 6 and 324 ± 8 µg/mL, respectively, equivalent to a 17- and 29-fold increase in solubility. This is attributed to the formation of relatively hydrophobic PDEA domains in the material, even below the LCST. The saturation solubility of tenofovir disoproxil fumarate was adversely affected in the thermoreversible gels, having values at 25 and 37 °C of 2582 ± 280 and 324 ± 8 µg/mL, respectively, equivalent to a 3- and 2-fold decrease, respectively. This decrease in solubility is partly explained by the reduced volume fraction of water but will also be a result of high solute concentration resulting in competition for hydration.

The release of progesterone or tenofovir disoproxil fumarate (50 µg/mL) from the A20-B10-A20 thermoreversible gel across cellulose membrane was investigated at both 25 and 37 °C (Figure 10). Progesterone release (Figure 9a) from the A20-B10-A20 thermoreversible gel at 25 °C followed Higuchi kinetics and 100 % of the drug was released after 32 h. The Higuchi model was applied to this release data as it is suitable for describing the release of both sparingly and abundantly soluble therapeutics from planar dosage forms.[45] This model is based on a linear fit to the fractional drug release with the square-root of time.[46] Increasing the temperature to 37 °C retarded the release of progesterone significantly, with 100 % drug liberated only after 144 h. This retardation of release at 37 °C is attributed to the formation of the gel phase, which provides microphase separated PDEA domains of relative hydrophobicity in which drug solubilisation may occur, disfavouring release. Additionally, increased tortuosity (i.e. a pathway having many turns) of the route taken by the drug for liberation within the gel

phase will contribute to retardation by ultimately increasing distance over which diffusion must occur. The progesterone release profile at 37 °C did not follow the Higuchi model, but its kinetics were linear after a 24 h lag period ($R^2 > 0.99$), which is highly attractive for controlled drug delivery releasing near-identical doses each day of use. The mechanisms for this zero-order behaviour can be rationalised by analogy to biphasic hydrogels containing hydrophilic polymer chains modified to possess hydrophobic moieties, as described by Varelas and co-workers.[47] In these systems where swollen hydrogels contain hydrophobic microdomains, hydrophobic drugs partition preferentially into the microdomains which act as reservoirs. On exposure to excess water of low solute concentration, the drug is released from the gel by diffusion through the bulk hydrogel phase, which is then restored to the bulk from the microdomain reservoirs. If the flux achieved by these two processes are comparable, the concentration of drug in the bulk hydrogel remains steady and the driving force for diffusion is at a pseudo-steady state and zero order release is possible. The release of tenofovir disoproxil fumarate from the thermoreversible gel was more rapid, with ca. 65 % drug release occurring after 8 h, and was unaffected by temperature. This has been reported for PNIPAM-*b*-PEG-*b*-PNIPAM gels, where it was hypothesised that the effect of increased tortuosity above T_{gel} is counteracted by increased thermal energy favouring diffusion across the membrane.[14] Furthermore, the relatively hydrophilic tenofovir is not expected to partition favourably into the phase separated PDEA domains, counteracting any reservoir effect.

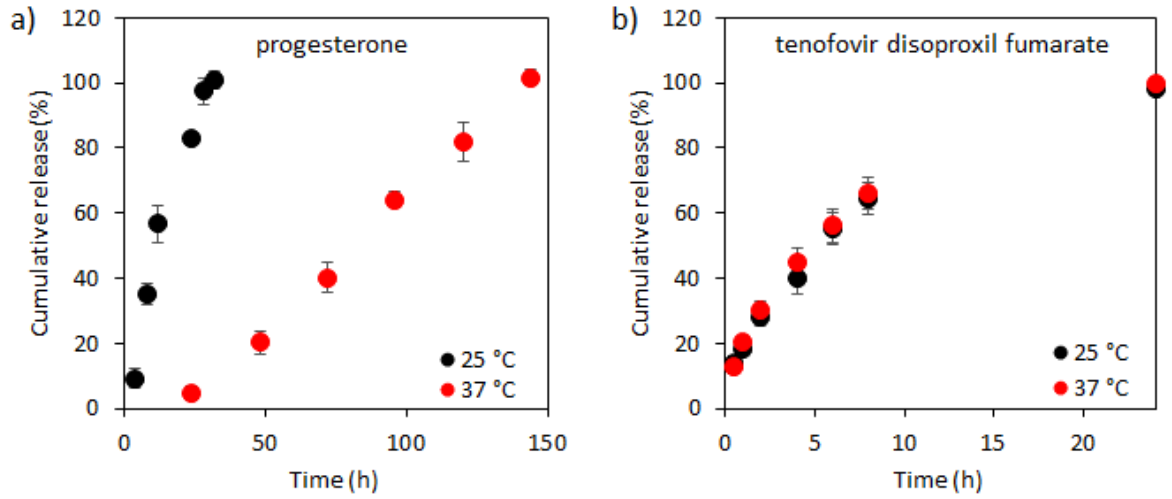

Figure 10. Release of progesterone (a) and tenofovir disoproxil fumarate (b) from A20-B10-A20 copolymer as a 30 % (w/v) solution in 0.3 M NaCl.

The potential of the A20-B10-A20 thermoreversible gels in vaginal drug delivery was further probed by assessing mucoadhesion using an established flow-through method.[28,48] In brief, fluorescein-doped samples were applied to the surface of *ex vivo* porcine vaginal mucosa and allowed to equilibrate at 37 °C, mimicking internal body temperature.[42] Simulated vaginal fluid was then washed over the surface of the mucosa and the presence of sample determined by fluorescence microscopy (Figure 11a). This retention can be quantified by the measurement of image pixel intensity with time (Figure 11b) to give a percentage of the fluorescence at time zero. The A20-B10-A20 thermoreversible gel was compared against Poloxamer 407 (20 wt%) as a widely used thermoreversible gel,[12,49,50] Poloxamer 188 (20 wt%) as a non-gel-forming polymer control, and fluorescein solution as a negative non-mucoadhesive control. The A20-B10-A20 thermoreversible gel could match the behaviour of Poloxamer 407 gel, giving non-significant differences in retention at the experiment end whilst having the benefit of T_{gel} closer to body temperature. The A20-B10-A20 thermoreversible gel outperformed the negative control and the Poloxamer 188 control, showing discrimination between mucoadhesive and non-mucoadhesive samples in the experiment. Future tuning of A20-B10-A20 construct could lead to a material that outperforms Poloxamer 407, either by further chemical modification of the copolymer to enhance covalent mucosa-polymer interactions (such as by thiol or maleimide chemistry)[51] or by formulation with mucoadhesive polymers.[52]

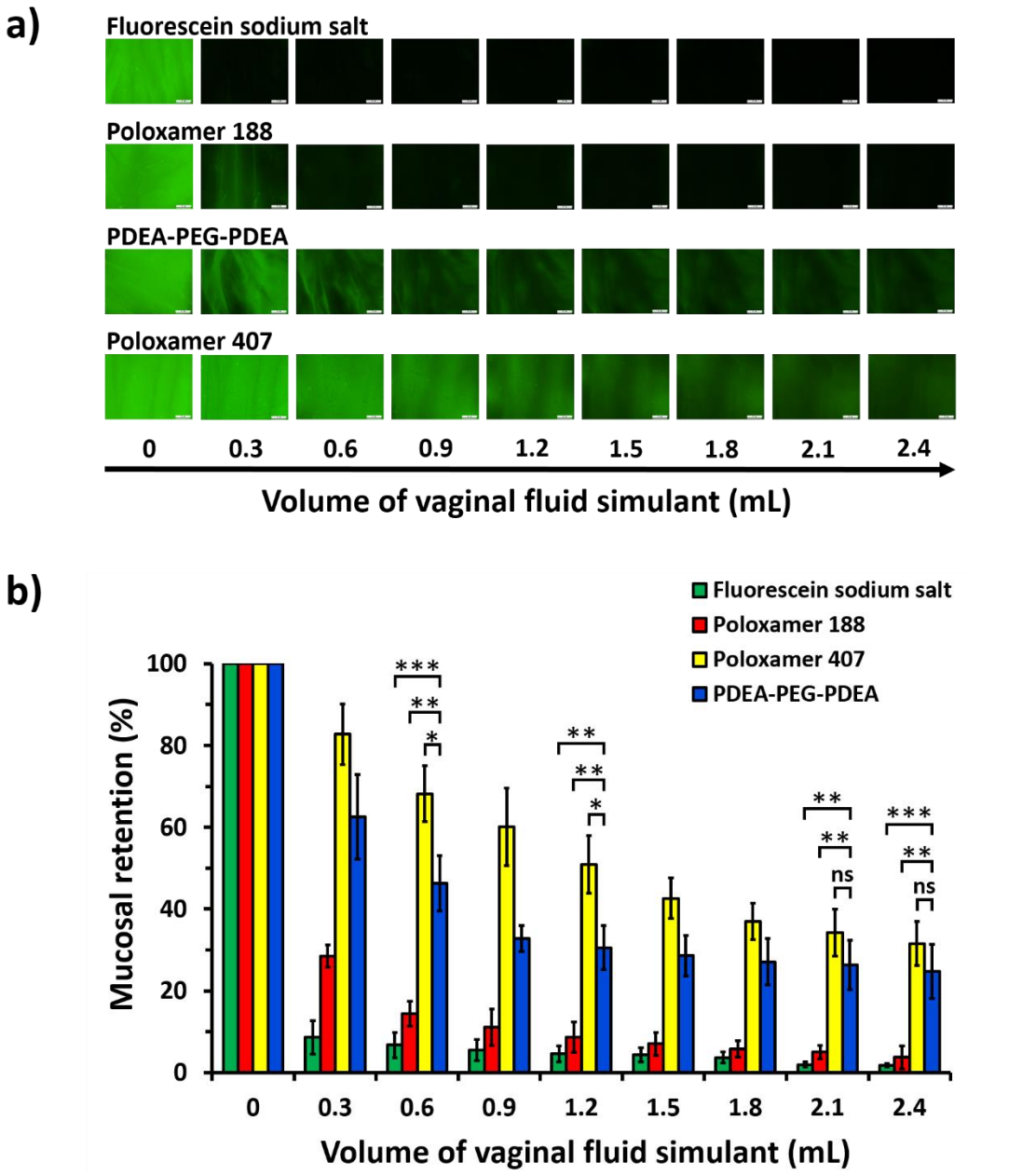

Figure 11. a) Selected fluorescence images showing retention of fluorescein sodium salt (NaFl), Poloxamer 188, PDEA-PEG-PDEA and Poloxamer 407 on freshly dissected porcine vaginal tissue washed with different volumes of VFS solution (flow rate 0.3 mL/min). Fluorescence microscope parameters: exposure time – 10 ms; gain – 1x, magnification – 16x. Scale bars are 2 mm. b) Percentage retention of fluorescein sodium salt (NaFl), Poloxamer 188 , Poloxamer 407 and PDEA-PEG-PDEA on freshly exiced porcine vaginal tissue after irrigating with different volumes of VFS solution (flow rate 0.3 mL/min). Data are expressed as mean ± standard deviation (n = 3). Statistically significant differences are given as: * = $p < 0.05$; ** = $p < 0.01$; *** = $p < 0.001$; ns = *no significance*.

4. Conclusions

Triblock copolymers with the structure PDEA-*b*-PEG-*b*-PDEA exhibit a temperature-dependent rheological response in aqueous solution, where heating above ca 35 °C induced an increase in viscosity. When heated, copolymer solutions with a 5 kDa central PEG blocks formed a viscous phase with dominance of a liquid-like behaviour (G″>G′), whereas constructs with 10 kDa PEG blocks formed gel phases with a predominantly solid-like behaviour (G′>G″). SAXS revealed that A10-B5-A10 copolymers (5 kDa central PEG) formed cylindrical nanostructures above the transition temperature, whereas A10-B10-A10 and A20-B10-A20 (10 kDa central PEG) formed spherical and elliptical aggregates, respectively; it is hypothesized that these aggregates are subsequently connected by long PEG chains forming bridges to form a percolating gel network. Combining rheology with cell culture studies led to the selection of A20-B10-A20 as the most promising thermoreversible gel for healthcare applications. Control of A20-B10-A20 concentration (30 % w/v) and ionic strength (0.3 M NaCl) allowed the gelation temperature to be manipulated to below 37 °C, enabling *in situ* gelation upon contact with the body's internal temperature, or warming during cell culture, for instance. This optimised material was highly-functional for topical drug delivery, enabling solubilisation of poorly water-soluble progesterone and releasing the drug over 6 days, as well as matching the performance of Poloxamer 407 in mucoadhesion studies.

Acknowledgements

The EPSRC (EP/T00813X/1) are thanked for funding the research of CAD, MAS, and MC via the New Investigator award. The Royal Society are also acknowledged for funding (RG160139). The University of Hertfordshire sponsored the PhD study of PH. We thank Daniel Nye from the Materials Characterization Laboratory at the ISIS Neutron and Muon source for his help with the SAXS measurements. DBK and VVK acknowledge the Ministry of Education and Science of the Republic of Kazakhstan (grant number AP08052780) for supporting experiments with retention of formulations on mucosal surfaces.

Supporting Information. Supporting Information is available from the Wiley Online Library or from the author.

Data availability statement. Data is available upon request to the corresponding author.

Received: ((will be filled in by the editorial staff))
Revised: ((will be filled in by the editorial staff))
Published online: ((will be filled in by the editorial staff))

References

[1] M. T. Cook, P. Haddow, S. B. Kirton, W. J. McAuley, *Adv. Funct. Mater.* **2021**, *31*, 2008123.

[2] M. A. Ward, T. K. Georgiou, *Polymers (Basel).* **2011**, *3*, 1215–1242.

[3] M. Hrubý, S. K. Filippov, P. Štěpánek, *Eur. Polym. J.* **2015**, *65*, 82–97.

[4] M. J. N. Junk, W. Li, A. D. Schlüter, G. Wegner, H. W. Spiess, A. Zhang, D. Hinderberger, *J. Am. Chem. Soc.* **2011**, *133*, 10832–10838.

[5] R. Suntornnond, J. An, C. K. Chua, *Macromol. Mater. Eng.* **2017**, *302*, 1–15.

[6] F. Doberenz, K. Zeng, C. Willems, K. Zhang, T. Groth, *J. Mater. Chem. B* **2020**, *8*, 607–628.

[7] L. D. Taylor, L. D. Cerankowski, *J Polym Sci Polym Chem Ed* **1975**, *13*, 2551–2570.

[8] I. Idziak, D. Avoce, D. Lessard, D. Gravel, X. X. Zhu, *Macromolecules* **1999**, *32*, 1260–1263.

[9] E. Ruel-Gariepy, J. C. Leroux, *Eur. J. Pharm. Biopharm.* **2004**, *58*, 409–426.

[10] R. Watanabe, K. Takaseki, M. Katsumata, D. Matsushita, D. Ida, M. Osa, *Polym. J.* **2016**, *48*, 621–628.

[11] S. A. Angelopoulos, C. Tsitsilianis, *Macromol. Chem. Phys.* **2006**, *207*, 2188–2194.

[12] M. A. Abou-Shamat, J. Calvo-Castro, J. L. Stair, M. T. Cook, *Macromol. Chem. Phys.* **2019**, *220*, 1900173.

[13] X. Zhang, T. F. Burton, M. In, S. Bégu, A. Aubert-Pouëssel, J. J. Robin, S. Monge, O. Giani, *Mater. Today Commun.* **2020**, *24*, 100987.

[14] P. Haddow, W. J. McAuley, S. B. Kirton, M. T. Cook, *Mater. Adv.* **2020**, *1*, 371–386.

[15] A. J. De Graaf, K. W. M. Boere, J. Kemmink, R. G. Fokkink, C. F. Van Nostrum, D. T. S. Rijkers, J. Van Der Gucht, H. Wienk, M. Baldus, E. Mastrobattista, T. Vermonden, W. E. Hennink, *Langmuir* **2011**, *27*, 9843–9848.

[16] C.-W. Chang, E. Bays, L. Tao, S. N. S. Alconcel, H. D. Maynard, *Chem. Commun.* **2009**, *0*, 3580.

[17] K. T. Nijenhuis, *Colloid Polym. Sci.* **1981**, *259*, 1017–1026.

[18] O. Glatter, O. Kratky, *Small Angle X-Ray Scattering*, Academic Press, **1982**.

[19] J. S. Pedersen, P. Schurtenberger, *Macromolecules* **1996**, *29*, 7602–7612.

[20] W.-R. Chen, P. D. Butler, L. J. Magid, *Langmuir* **2006**, *22*, 6539–6548.

[21] D. I. Svergun, M. H. J. Koch, P. A. Timmins, R. P. May, *Small Angle X-Ray and Neutron Scattering from Solutions of Biological Macromolecules*, Oxford University Press, **2013**.

[22] A. Isihara, *J. Chem. Phys.* **1950**, *18*, 1446–1449.

[23] A. Guinier, G. Fournet, *Small-Angle Scattering of x-Rays*, University Microfilms International, Ann Arbor, Mich; London, **1979**.

[24] J. K. Percus, G. J. Yevick, M. Kotlarchyk, S. H. Chen, *Phys. Rev.* **1958**, *110*, 1–13.

[25] M. Kotlarchyk, S. H. Chen, *J. Chem. Phys.* **1983**, *79*, 2461–2469.

[26] J. K. Percus, G. J. Yevick, *Phys. Rev.* **1958**, *110*, 1.

[27] M. T. Cook, S. L. Smith, V. Khutoryanskiy, *Chem. Commun.* **2015**, *51*, 14447–14450.

[28] C. A. Withers, M. T. Cook, L. Methven, M. a Gosney, V. V Khutoryanskiy, *Food Funct.* **2013**, *4*, 1668–74.

[29] A. N. Semenov, J. F. Joanny, A. R. Khokhlov, *Macromolecules* **1995**, *28*, 1066–1075.

[30] S. K. Filippov, A. Bogomolova, L. Kaberov, N. Velychkivska, L. Starovoytova, Z. Cernochova, S. E. Rogers, W. M. Lau, V. V. Khutoryanskiy, M. T. Cook, *Langmuir* **2016**, *32*, 5314–5323.

[31] E. D. H. Mansfield, S. K. Filippov, V. R. de la Rosa, M. T. Cook, I. Grillo, R.

Hoogenboom, A. C. Williams, V. V. Khutoryanskiy, *J. Colloid Interface Sci.* **2021**, *590*, 249–259.

[32] S. M. King, in *Mod. Tech. Polym. Characterisation* (Eds.: R.A. Pethrick, J. Dawkins), John Wiley & Sons, Ltd, **1999**, pp. 171–232.

[33] A. Blanazs, S. P. Armes, A. J. Ryan, *Macromol. Rapid Commun.* **2009**, *30*, 267–277.

[34] M. A. da Silva, P. Haddow, S. B. Kirton, W. J. McAuley, L. Porcar, C. A. Dreiss, M. T. Cook, *Submitt. (undergoing Revis. Follow. Rev.* **2021**.

[35] C. A. Dreiss, *Soft Matter* **2007**, *3*, 956–970.

[36] M. Teodorescu, I. Negru, P. O. Stanescu, C. Drăghici, A. Lungu, A. Sârbu, *React. Funct. Polym.* **2010**, *70*, 790–797.

[37] I. Negru, M. Teodorescu, P. O. Stanescu, C. Draghici, A. Lungu, A. Sarbu, *Mater. Plast.* **2010**, 35–41.

[38] H. H. Lin, Y. L. Cheng, *Macromolecules* **2001**, *34*, 3710–3715.

[39] A. P. Constantinou, N. F. Sam-Soon, D. R. Carroll, T. K. Georgiou, *Macromolecules* **2018**, *51*, 7019–7031.

[40] A. P. Constantinou, T. Lan, D. R. Carroll, T. K. Georgiou, *Eur. Polym. J.* **2020**, *130*, 109655.

[41] H. Du, R. Wickramasinghe, X. Qian, *J. Phys. Chem. B* **2010**, *114*, 16594–16604.

[42] M. T. Cook, M. B. Brown, *J. Control. Release* **2018**, *270*, 145–157.

[43] K. S. Merriam, K. A. Leake, M. Elliot, M. L. Matthews, R. S. Usadi, B. S. Hurst, *Int. J. Endocrinol.* **2015**, *2015*, DOI 10.1155/2015/685281.

[44] J. M. Smith, R. Rastogi, R. S. Teller, P. Srinivasan, P. M. M. Mesquita, U. Nagaraja, J. M. McNicholl, R. M. Hendry, C. T. Dinh, A. Martin, B. C. Herold, P. F. Kiser, *Proc. Natl. Acad. Sci. U. S. A.* **2013**, *110*, 16145–16150.

[45] M. L. Bruschi, in *Strateg. to Modify Drug Release from Pharm. Syst.*, **2015**.

[46] S. Dash, P. N. Murthy, L. Nath, P. Chowdhury, *Acta Pol. Pharm. - Drug Res.* **2010**, *67*, 217–223.

[47] C. G. Varelas, D. G. Dixon, C. A. Steiner, *J. Control. Release* **1995**, *34*, 185–192.

[48] R. A. Cave, J. P. Cook, C. J. Connon, V. V Khutoryanskiy, *Int. J. Pharm.* **2012**, *428*, 96–102.

[49] S. F. Khattak, S. R. Bhatia, S. C. Roberts, *Tissue Eng.* **2005**, *11*, 974–83.

[50] G. Niu, F. Du, L. Song, H. Zhang, J. Yang, H. Cao, Y. Zheng, Z. Yang, G. Wang, H. Yang, S. Zhu, *J. Control. Release* **2009**, *138*, 49–56.

[51] R. P. Brannigan, V. V. Khutoryanskiy, *Macromol. Biosci.* **2019**, *19*, 1–11.

[52] R. R. de Araújo Pereira, J. S. Ribeiro Godoy, T. I. Stivalet Svidzinski, M. L. Bruschi, *J. Pharm. Sci.* **2013**, *102*, 1222–1234.

Supplementary Information

Methods

Preparation of vaginal fluid simulant

Vaginal fluid simulant (VFS) was prepared according to the previously reported protocol [*Derek H. Owen and David F. Katz. A vaginal fluid simulant. Contraception 1999, 59, 91-95*]. The recipe for 1 L preparation of vaginal fluid simulant (VFS) in deionised water:

Compound name	**Amount (g)**
Sodium chloride (NaCl)	3.51 g (0.060 mol)
Potassium chloride (KOH)	1.40 g (0.025 mol)
Calcium chloride ($Ca(OH)_2$)	0.222 g (0.003 mol)
Bovine serum albumin	0.018 g
Lactic acid	2.0 g (0.022 mol)
Acetic acid	1.0 g (0.011 mol)
Glycerol	0.16 g (0.002 mol)
Urea	0.40 g (0.007 mol)
Glucose	5.0 g (0.028 mol)

The solution is adjusted to pH 4 with 1 M HCl.

Table S1. Feed mixtures for polymerisations

Tri-block Copolymer	Monomer (Quantity)	Initiator (Quantity)	Catalyst (Quantity)	Ligand (Quantity)	Solvent (Quantity)	Temp (°C)	Yield (%)
A10-B5-A10	DEA (5.4 mL, 39.3 mmol)	PEG_{5kDa} (0.5 g, 125 µmol)	CuBr (35.9 mg, 250 µmol)	Me_6TREN (66.8 µL, 250 µmol)	MeOH: Water (1:1) (20 mL)	RT	92.3
A20-B5-A20	DEA (8.1 mL, 59.0 mmol)	PEG_{5kDa} (0.5 g, 125 µmol)	CuBr (35.9 mg, 250 µmol)	Me_6TREN (66.8 µL, 250 µmol)	MeOH: Water (1:1) (20 mL)	RT	91.6
A10-B10-A10	DEA (4.3 mL, 31.5 mmol)	PEG_{10kDa} (1.0 g, 100 µmol)	CuBr (28.7 mg, 200 µmol)	Me_6TREN (53.5 µL, 200 µmol)	MeOH: Water (1:1) (20 mL)	RT	88.2
A20-B10-A20	DEA (6.5 mL, 47.3 mmol)	PEG_{10kDa} (1.0 g, 100 µmol)	CuBr (28.7 mg, 200 µmol)	Me_6TREN (53.5 µL, 200 µmol)	MeOH: Water (1:1) (20 mL)	RT	86.0

Table S2. Molecular weight and polydispersity of PDEA-*b*-PEG-*b*-PDEA copolymers.

Polymer ID	**M_n by ^1H NMR (kDa)**	**M_n of PDEA by ^1HNMR (kDa)**	**Đ (GPC)**
A10-B5-A10	31	13	1.40
A20-B5-A20	47	21	1.35
A10-B10-A10	36	13	1.18
A20-B10-A20	53	21	1.32

Table S3. Fitting parameters of SAXS data for the A10-B5-A10 copolymer. Cyl = Cylinder form factor, PGC = polydisperse Gaussian coil form factor

Temp (°C):	30	37	40	50	60
Model	PGC	PGC	Cyl+PL	Cyl	Cyl
Cylinder length (Å)			1000	1000	1000
Radius of the cross-section (Å)			62	91	87
$SLD_{scatterer}$ (10^{-6} Å^{-2})			9.40	9.40	9.40
$SLD_{solvent}$ (10^{-6} Å^{-2})			9.20	9.20	9.20
I_0 (cm^{-1})	0.0062	0.0108			
Radius of Gyration (Å)	48.55	98.34			
Polymer polydispersity	2.00	2.00			
Radius polydispersity			0.20	0.20	0.20
Power Law exponent			1.60		

Table S4. Fitting parameters of SAXS data for the A10-B10-A10 copolymer. Sp = Sphere form factor, Ep = Elliptical form factor, HSp = hard sphere structure factor.

Temp (°C):	30	37	40	50	60
Model	PGC	PGC	Ep+PGC	SpHSp	SpHSp
Polar radius (Å)			205	129	137
Equatorial radius (Å)			102		
$SLD_{scatterer}$ (10^{-6} Å^{-2})			9.2	9.2	9.2
$SLD_{solvent}$ (10^{-6} Å^{-2})			9.4	9.4	9.4
Effective radius (Å)				216	211
Correlated volume fraction				0.12	0.11
I_0 (cm^{-1})	0.0065	0.0089	0.0080		
Radius of Gyration (Å)	44.49	70.63	73.38		
Polymer polydispersity	2.00	2.00	2.00		
Radius polydispersity				0.20	0.20
Radius polydispersity				0.20	0.20
Polar radius polydispersity			0.20		

Equatorial radius polydispersity			0.20		

Table S5. Fitting parameters of SAXS data for the A20-B10-A20 copolymer. HSp = hard sphere structure factor, PGC = polydisperse Gaussian coil form factor.

Temp (°C):	30	37	40	50	60
Model	PGC	Ep+PGC	EpHSp+PGC	EpHSp	EpHSp
Polar radius		262	275	285	278
Equatorial radius		113	157	191	193
$SLD_{scatterer}$ (10^{-6} Å^{-2})		9.2	9.2	9.2	9.2
$SLD_{solvent}$ (10^{-6} Å^{-2})		9.4	9.4	9.4	9.4
Effective radius (Å)			264	286	282
Correlated volume fraction			0.07	0.11	0.09
I_0 (cm^{-1})	0.0073	0.074	0.0053		
Radius of Gyration (Å)	63.10	40.00	45.27		
Polymer polydispersity	2.00	2.00	2.00		
Polar radius polydispersity			0.20	0.05	0.05
Equatorial radius polydispersity			0.20	0.05	0.05

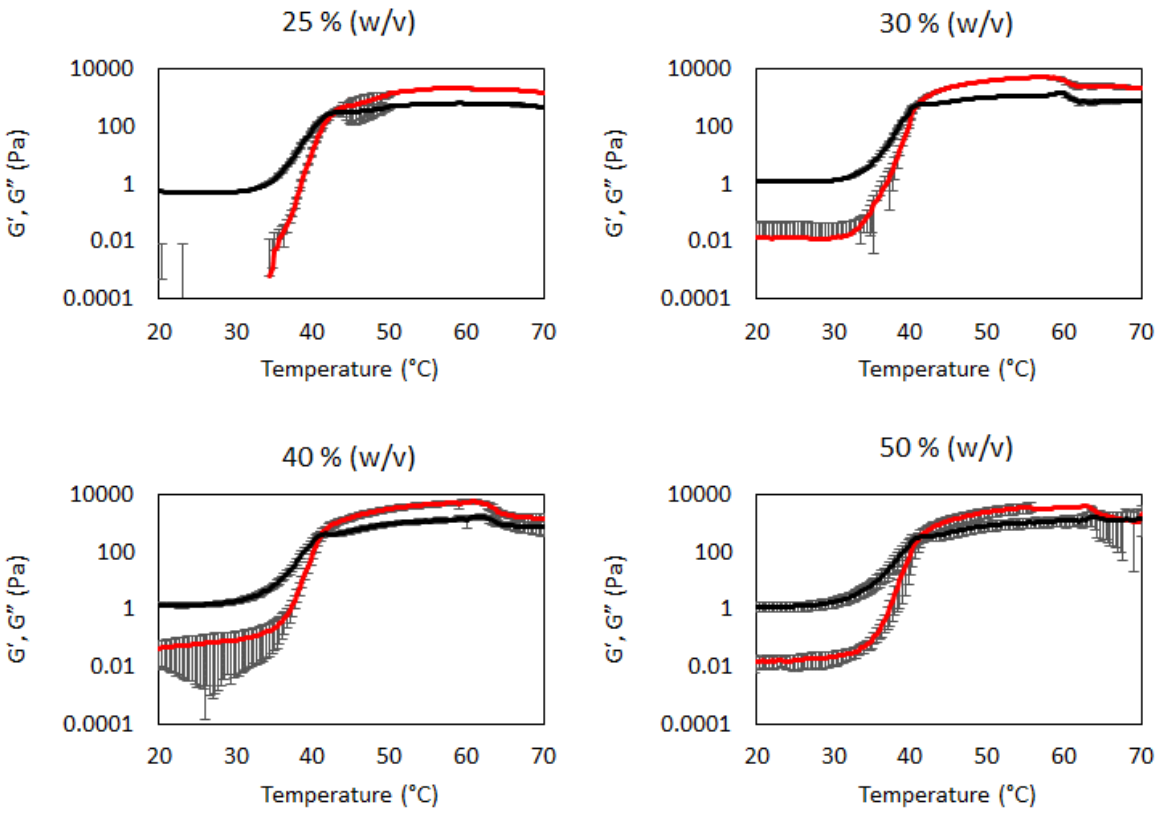

Figure S1. Rheometric temperature ramps of 25-50 % (w/v) aqueous solutions of A20-B10-A20, with G′ shown in red and G″ in black. Rheometry was conducted at 1 Hz and 1 Pa in triplicate. Data presented as mean ± standard deviation.

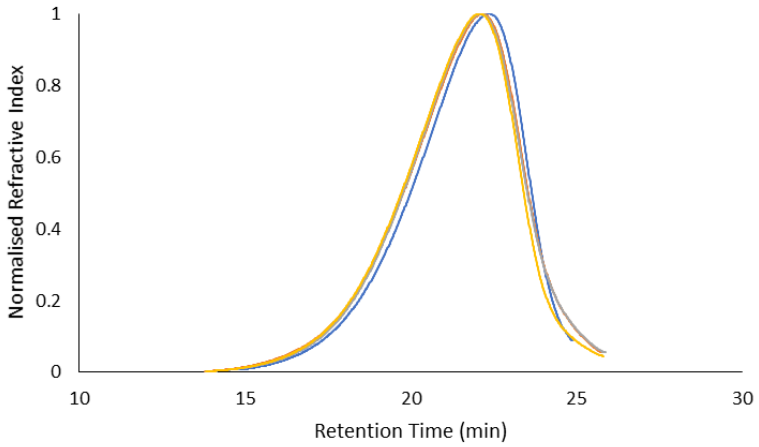

Figure S2. GPC traces of A20-B10-A20 after storage in solution at week 0 (blue) and week 12 at 4 (red), 25 (grey) and 40 °C (yellow).